
CONVOLUTIONAL SIGNATURE FOR SEQUENTIAL DATA ^{*}

Ming Min [†]Tomoyuki Ichiba [‡]

September 16, 2020

ABSTRACT

Signature is an infinite graded sequence of statistics known to characterize geometric rough paths, which includes the paths with bounded variation. This object has been studied successfully for machine learning with mostly applications in low dimensional cases. In the high dimensional case, it suffers from exponential growth in the number of features in truncated signature transform. We propose a novel neural network based model which borrows the idea from Convolutional Neural Network to address this problem. Our model reduces the number of features efficiently in a data dependent way. Some empirical experiments are provided to support our model.

1 Introduction

Multi-dimension sequential data analysis has become an import research area in machine learning, financial mathematics and many other area. In convention, there are several methods for analyzing sequential data. In deep learning, people have already developed recurrent neural network (RNN), such as LSTM [11] and other forms of RNN [6]. They have been successfully applied into a variety of tasks, such as natural language processing, financial time series, medical data and so on. Another approach is to use Bayesian learning, mostly involved with Gaussian Process [27]. By pre-determine a priori distribution, GP has advantage in quantifying uncertainty. For example, [25] use GP to solve PDE with noisy boundary observations. Recently, people proposed a novel mathematical object, called signature of a path, and use it to summarize information of path data, see [3, 5, 15, 20, 21].

Signature is a graded feature set of a stream, or sequential data, which is derived from the Rough Path theory. As a feature map, signature has been introduced into the machine learning field with the application in sequential data successfully. This special feature set has universality and can be used to characterize path data efficiently with truncation. The efficiency is understood as summarizing the high frequency sequential data into several features by truncated signature in the case of low dimensional path. Signature has been used broadly in these cases. [19] use signatures to characterize high frequency trading paths. [12] use signature transform as a layer of neural network, and proposed the deep signature transform model. Moreover, using signature is model free, data dependent, see [17, 18].

However, the number of features in the truncated signature suffers from exponential growth with respect to the dimension. In the case of high dimensional sequential data, this feature map becomes problematic. A kernel based learning algorithm has been introduced to address this problem, see [14, 26]. In this paper, we propose a new algorithm to solve this problem by combining Convolutional Neural Network and signature transform. We show by experiments in this paper that this algorithm can be very efficient. This algorithm may contribute to many applications of signatures in the cases of high dimensional sequential data.

The rest of this paper is organized as follows. In Section 2, we introduce the signature of a rough path, geometric rough path and some nice properties of signature, and discuss classification problems by using signature. In Section 3, we introduce the main algorithm of this paper, Convolutional Signature model, discuss how this model reduces the number of features and show that this model preserves all information of path data. In Section 4, a broad range of

^{*} Work is supported by NSF grant DMS-2008427 for the second author.

[†]Department of Statistics and Applied Probability, South Hall, University of California, Santa Barbara, CA 93106, USA (E-mail: m_min@pstat.ucsb.edu).

[‡]Department of Statistics and Applied Probability, South Hall, University of California, Santa Barbara, CA 93106, USA (E-mail: ichiba@pstat.ucsb.edu).

experiments are done to support our model, including high dimensional time series classification, functional estimation and textual sentimental detection. We conclude and explain further ongoing research in Section 5.

2 Signature and Geometric Rough Paths

2.1 Signatures

First let us specify some notations, following [21]. Given a Banach space E whose norm is denoted by $\|\cdot\|$, we define the tensor algebra

$$T((E)) := \{(a_i)_{i \geq 0} : a_i \in E^{\otimes i} \text{ for every } i\}.$$

This $T((E))$ is an algebra with the sum $+$, given by

$$(a_i)_{i \geq 0} + (b_i)_{i \geq 0} := (a_i + b_i)_{i \geq 0}, \quad \forall (a_i)_{i \geq 0}, (b_i)_{i \geq 0} \in T((E)),$$

and with the tensor product \otimes , given by

$$(a_i)_{i \geq 0} \otimes (b_i)_{i \geq 0} := (c_i)_{i \geq 0}, \quad \forall (a_i)_{i \geq 0}, (b_i)_{i \geq 0} \in T((E)),$$

where c_i is the convolution $c_j := \sum_{k=0}^j a_k \otimes b_{j-k}$ of the first j elements of $(a_i)_{i \geq 0}$ and $(b_i)_{i \geq 0}$ for $j \geq 0$.

Similarly, let us define its subset

$$T(E) := \{(a_i)_{i \geq 0} : a_i \in E^{\otimes i} \text{ and } \exists N \in \mathbb{N} \text{ such that } a_i = 0 \forall i \geq N\}$$

of $T((E))$ for those with finite number of non-zero elements. Also, for the purpose of computational efficiency, we shall consider truncated tensor algebra of order $m \in \mathbb{N}$, that is,

$$T^m(E) := \{(a_i)_{i=0}^m : a_i \in E^{\otimes i} \text{ for } \forall i \leq m\},$$

which is a subalgebra of $T((E))$. Then as we shall see, our signatures and truncated signatures will lie in these spaces $T((E))$ and $T^m(E)$, respectively.

Now with $E := \mathbb{R}^d$ and the usual Euclidean norm $\|\cdot\|$, we shall define the space $\mathcal{V}^p([0, T], E)$ of the d -dimensional continuous paths of finite p -th variation over the time interval $[0, T]$ and the signature of the path in $\mathcal{V}^p([0, T], E)$.

Definition 2.1 (The space of finite p -variation). *Let $p \geq 1$, $X : [0, T] \rightarrow E := \mathbb{R}^d$ be a d -dimensional path, $D := \{t_i\}_{1 \leq i \leq n}$ is a partition of $[0, T]$ with $0 = t_0 < t_1 < \dots < t_n$. Then the p -variation of X is defined by*

$$\|X\|_p := \left(\sup_{D \subset [0, T]} \sum_{i=0}^{n-1} \|X_{t_{i+1}} - X_{t_i}\|^p \right)^{1/p}.$$

X is said to be of finite p -variation if $\|X\|_p < \infty$, and we denote the set of any continuous path $X : [0, T] \rightarrow E$ of finite p -variation by $\mathcal{V}^p([0, T], E)$.

Example 2.1 (Smooth paths and piece-wise linear paths). *We give 2 examples of paths in $\mathcal{V}^p([0, T], E)$, as shown in Figure 1. In the left panel, we plot the smooth path $X_t = (t, (t-2)^2), t \in [0, 4]$. In the right panel, we use discrete data: daily AAPL adjusted close stock price from Nov 28, 2016 to Nov 24, 2017, and then interpolate the path linearly between each successive two days.*

We define the supremum norm $\|\cdot\|_\infty$ for continuous functions. If we equip the space $\mathcal{V}^p([0, T], E)$ with the norm $\|X\|_{\mathcal{V}^p([0, T], E)} := \|X\|_p + \|X\|_\infty$, then $\mathcal{V}^p([0, T], E)$ is a Banach space.

Then signature of path X is given as follows.

Definition 2.2 (Signatures). *Let $p \geq 1$, the signature of a path $X \in \mathcal{V}^p([0, T], E)$ is defined as*

$$S(X) := (1, X^1, X^2, \dots) \in T((E))$$

where $X^k := \int \dots \int_{0 < t_1 < \dots < t_n < T} dX_{t_1} \otimes \dots \otimes dX_{t_n} \in E^{\otimes k}$ is defined by the k -fold, iterated integral for $k \geq 1$, provided that the iterated integrals make sense. The truncated signature is naturally defined as $S^m(X) := (1, X^1, X^2, \dots, X^m) \in T^m(E)$ for every m .

Remark 2.1. *The integral depends on the nature of paths. Here are some examples.*

1. *If X is of 1-variation path, then the integral of signature can be understood as the Stieltjes integral;*
2. *If X is of p -variation path with $1 < p < 2$, then the integral can be defined in the sense of Young [20].*
3. *If X is a Brownian motion, then we can use the Itô integral or Stratonovich integral.*

As we will explain later, if we want to extend a Brownian motion path or semimartingale to a geometric rough path, then we have to choose the Stratonovich integral rather than the Itô integral.

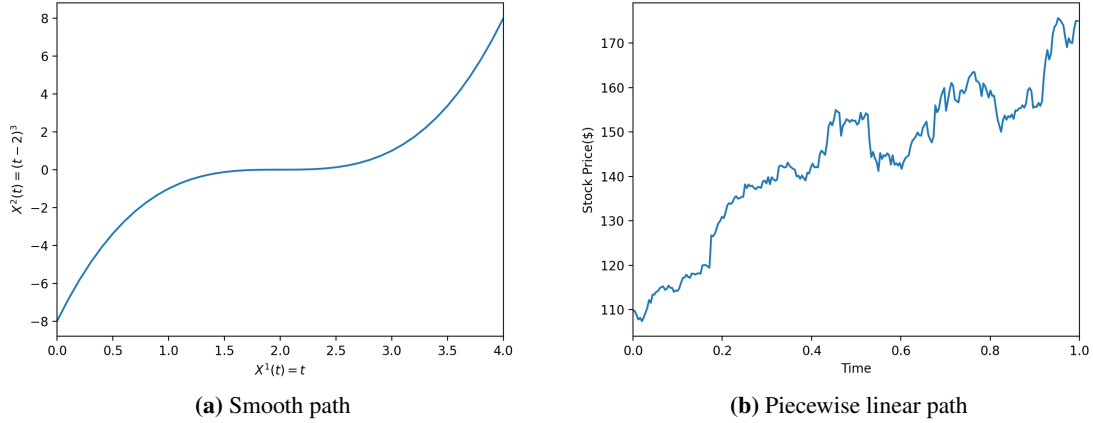


Figure 1: (a) Plot of a smooth path $X_t = (t, (t-2)^2)$, $t \in [0, 4]$. (b) Plot of linear interpolation of daily AAPL adjusted close stock price from Nov 28, 2016 to Nov 24, 2017.

2.2 Geometric Rough Paths and Linear Functionals

Here we introduce rough paths and geometric rough paths briefly. More details can be found in [20] and [21]. Instead of $T((E))$, p -rough paths and geometric p -rough paths are objects in $T^{[p]}(E)$ for some $p(\geq 1)$. A fundamental result from rough paths theory is that there exists a continuous unique lift from $T^{[p]}(E)$ to $T((E))$. This lift is done in an iterated integral way and gives us the signature of rough paths. We denote the space of p -rough paths by Ω_p . The space of geometric p -rough paths, $G\Omega_p$, is defined by the p -variational closure of $S^{[p]}(\Omega_1)$. For path $X : [0, T] \rightarrow \mathbb{R}^d$ with bounded p -variation, $S^{[p]}(X) \in \Omega_p$. If X is of bounded 1-variation, then $S^{[p]}(X) \in G\Omega_p$ for any $p(\geq 1)$.

Signature enjoys many nice properties. For example, signature characterize paths up to tree-like equivalence [3] that are parametrisation invariant.

Proposition 2.1 (Parametrisation Invariance). *Let $X : [0, T] \rightarrow \mathbb{R}^d$ be a path and $\psi : [0, T] \rightarrow [0, T]$ a reparametrization. Define \tilde{X} by $\tilde{X}_t = X_{\psi(t)}$, then each term in $S(\tilde{X})$ is equal to the corresponding term in $S(X)$, i.e. $S(\tilde{X}) = S(X)$.*

Moreover, if there exists a monotone increasing dimension in the path with bounded variation or geometric rough path, we can get rid of tree-like equivalence ([3], [10] and [15]). Parametrisation invariance can also be avoided by including time stamps as the extra dimension. In other words, provided that an extra time dimension included, signature characterize geometric rough path uniquely. Another useful fact of signature from rough path theory [20], [5] is that signature terms enjoy a factorial decay as the depth increasing, which makes truncating signature reasonable. The following example shows the factorial decay for bounded 1-variation paths.

Example 2.2 (Factorial Decay, [21] Prop 2.2). *Let $X : [0, T] \rightarrow \mathbb{R}^d$ be a continuous path with bounded 1-variation, then*

$$\left\| \int_{0 \leq t_1 < \dots < t_k \leq T} dX_{t_1} \otimes \dots \otimes dX_{t_k} \right\| \leq \frac{\|X\|_1^k}{k!}, \quad (2.1)$$

where $\|\cdot\|$ is tensor norm.

All these properties drive us to use signature as a feature map in Data Science. We shall then define linear forms on signatures.

For simplicity, let us fix E be an \mathbb{R}^d , and $\{e_i\}_{i=1}^d$ be a basis of \mathbb{R}^d . Then $\{e_i^*\}_{i=1}^d$ forms a basis of the dual space of \mathbb{R}^d , i.e. $(\mathbb{R}^d)^*$. For every $n \in \mathbb{N}$, $(e_{i_1}^* \otimes \dots \otimes e_{i_n}^*)$ can be naturally extended to $(E^*)^{\otimes n}$ with the basis $(e_I^* = e_{i_1}^* \otimes \dots \otimes e_{i_n}^*)$, where $i_k \in \{1, 2, \dots, d\}$ and we call $I = i_1 \dots i_n$ a word. The linear actions of $(E^*)^{\otimes n}$ on $E^{\otimes n}$ extends naturally a linear mapping $(E^*)^{\otimes n} \rightarrow T((E))^*$ by

$$e_I^*(\mathbf{a}) = e_I^*(a_n),$$

for every I and every $\mathbf{a} = (a_0, a_1, \dots, a_n, \dots) \in T((E))$.

Let A^* be the collection of all words for all $n \in \mathbb{N}$. Then $\{e_I^*\}_{I \in A^*}$ forms a basis of $T((\mathbb{R}^d)^*)$. Let $I, J \in A^*$ be two words with $I = i_1 \dots i_m$ and $J = j_1 \dots j_n$. We say a permutation σ in the symmetric group \mathfrak{S}_{m+n} is a *shuffle* of $\{1, \dots, m\}$ and $\{m+1, \dots, m+n\}$ if $\sigma(1) < \dots < \sigma(m)$ and $\sigma(m+1) < \dots < \sigma(m+n)$. We denote the collection of all *shuffle* by $Shuffles(m, n)$.

Definition 2.3 (Shuffle Product). The shuffle product of e_I^* and e_J^* denoted by $e_I^* \sqcup e_J^*$ is defined below:

$$e_I^* \sqcup e_J^* = \sum_{\sigma \in \text{Shuffles}(m, n)} e_{(k_{\sigma^{-1}(1)} \cdots k_{\sigma^{-1}(m+n)})}^*, \quad (2.2)$$

where $I = i_1 \cdots i_m$, $J = j_1 \cdots j_n$ and $k_1 \cdots k_{m+n} = i_1 \cdots i_m j_1 \cdots j_n$.

Denote $T((\mathbb{R}^d))^*$ as the space of linear forms on $T((\mathbb{R}^d))$ induced by $T((\mathbb{R}^d)^*)$. The shuffle product between $f, g \in T((\mathbb{R}^d))^*$ denoted by $f \sqcup g$ can be defined via natural extension of (2.2) according to bilinearity of \sqcup .

$T((\mathbb{R}^d))^*$ can be proved to be an algebra equipped with shuffle product and element-wise addition restricted to the space $S(\mathcal{V}^p([0, T], \mathbb{R}^d))$, see [21] Theorem 2.15. The following theorem motivates us to use signature as a feature map.

Proposition 2.2. Let $p \geq 1$, and let $f : \mathcal{V}^p([0, T], \mathbb{R}^d) \rightarrow \mathbb{R}$ be a continuous function on the path. Given that a compact subset K of $\mathcal{V}^p([0, T], \mathbb{R}^d)$, if $S(x)$ is a p -geometric rough path for each $x \in K$, then for $\forall \epsilon > 0$, there exist a linear forms $l^\epsilon \in T((\mathbb{R}^d))^*$, such that

$$\sup_{x \in K} |f(x) - \langle l^\epsilon, S(x) \rangle| < \epsilon.$$

Proof. The proof follows from the uniqueness of signature transform for geometric rough paths and the Stone-Weierstrass theorem. Please see Theorem 4.2 in [1] for more details. \square

Since the truncated signature $S^m(X) \in T^m(\mathbb{R}^d)$ has $\sum_{k=0}^m d^k = \frac{d^{m+1}-1}{d-1}$ many terms, the signature transform is an efficient feature reduction technique when we have the d dimensional path sampled with high frequency in time. However, when d is large, the number of signature terms increase exponentially and make signature not applicable in practical. To our knowledge at this time, only [14] introduce a new algorithm of calculating kernel of signatures and [26] discuss the application of kernel methods to fix this problem. We introduce Convolutional Neural Network (CNN) to solve this problem in Section 3.

2.3 Classification via Signature

In classification problems, we estimate the probability of an object belonging to each class. This estimation problem can be solved via signature for sequential data classification.

Let $(\Omega, \mathbb{P}, \mathcal{F})$ be a probability space. Suppose we have k classes, class 1, class 2, ..., class k , and N paired independent data $(x^n, y^n)_{1 \leq n \leq N}$, where $x^n : [0, T] \rightarrow \mathbb{R}^d$ is the path data and the corresponding label $y^n \in \{1, \dots, k\}$ of the class. Since the path data is often observed at discrete time stamps and we use piece-wise linear interpolations to connect them, it is reasonable to assume that x is of bounded 1-variation. Hence, $S(x^n)$ is a geometric 1 rough path.

Our sequential classification problem is stated as follows: given training data $(x^n, y^n)_{1 \leq n \leq N}$, derive a classifier g for predicting the labels for unseen data (x, y) . Let $p_i(x) := \mathbb{P}(y = i|x)$ for $i \in \{0, 1, \dots, k\}$, our goal is to estimate these $p_i(x)$. Since $S(x)$ determines x uniquely, it is reasonable to consider $S(x)$ and a nonlinear continuous function $g : T((\mathbb{R}^d)) \rightarrow [0, 1]^k$, such that

$$g(S(x)) = (\hat{p}_1(x), \dots, \hat{p}_k(x))^T, \quad (2.3)$$

where \hat{p}_i 's are estimator of p_i 's, subject to $\sum_{i=1}^k \hat{p}_i(x) = 1$.

For practical use, we use the truncate signature transforms thanks to the factorial decay property of the signature. Suppose we are using depth m , denote the corresponding linear function as l^m , then we obtain the estimate

$$g(S^m(x)) = (\hat{p}_1(x), \dots, \hat{p}_k(x))^T, \quad (2.4)$$

where $g : T^m(\mathbb{R}^d) \rightarrow [0, 1]^k$ and then the predicted label is given by

$$\hat{y} = \arg \max_i \hat{p}_i(x). \quad (2.5)$$

Example 2.3 (GARCH time series). We give an example of two classes of time series, $\{x^n\}_{n=1}^N$, generated by GARCH(2,2) model. The time series are given by

$$\begin{aligned} x_k^i &= \sigma_k \epsilon_k, \\ \sigma_k^2 &= w + \sum_{l=1}^2 \alpha_l x_{k-l}^i + \sum_{j=1}^2 \beta_j \sigma_{k-j}^2, \end{aligned}$$

where $w > 0$, $\alpha_i \geq 0$, $\beta_j \geq 0$ and ϵ_k 's are I.I.D. standard normal distributed. Denote $\alpha = (\alpha_1, \alpha_2)$ and $\beta = (\beta_1, \beta_2)$. 2 classes of GARCH time series are generated by setting parameters in Table 1.

For paths x^i generated by the first row parameters, we label $y^i = 1$, for the rest paths x^i generated by the second row parameters, we label them by $y^i = 2$. Thus, we generate paired data $\{(x^i, y^i)\}_{i=1}^N$.

class	w	α	β
1	0.5	(0.4, 0.1)	(0.7, 0.5)
2	0.2	(0.8, 0.5)	(0.4, 0.1)

Table 1: Parameters for GARCH(2,2) time series.

Remark 2.2. We cannot apply Proposition 2.2 here, because this $p(x)$ may not be continuous in x . Intuitively, it is better to add nonlinearity on $g(\cdot)$. The experiment in Section 4.2 verifies this intuition.

In practice, (2.4) and (2.5) are used and the goal is to find the classification model $g(\cdot)$ to estimate \hat{y} . In Section 4, we apply the logistic regression to Example 2.3 and the result shows that using truncated signature to classify this GARCH(2,2) time series is significantly efficient.

3 Convolutional Signature Model

The main goal of this section is to introduce the Convolutional Signature (CNN-Sig) model. As we have seen in Section 2.2, the truncated signature suffers from exponential growth when the dimension d is large, and in this case both space and time complexity increase dramatically. We will use Convolutional Neural Network(CNN) to reduce this exponential growth to at most linear growth. CNN has been mostly used in analyzing visual imagery, where it takes advantage of the hierarchical pattern in picture data and assembles complex pattern by focusing on small piece of the picture. Convolutional layer convolves the input data with a small rectangular kernel, and the output data can be masked with an activation function. We believe that there are some patterns between channels of a path, this motivates us to consider signature with CNN to address the high dimensional problem.

Before introducing the CNN-Sig model, we shall explain that the signature transform can be viewed as a layer in deep neural network model.

3.1 Signature as a Layer

Signature can be viewed as a layer. In the background of Python package **signatory** [13], signature transform takes input tensor of shape (b, n, d) , corresponding to a batch of size b of paths in \mathbb{R}^d with n observing points at time $\{t_j\}_{j=1}^n$, and returns a tensor of shape $(b, \frac{d^{m+1}-d}{d-1})$ or a stream like tensor of shape $(b, n, \frac{d^{m+1}-d}{d-1})$. Usually it omits the first term 1 for the signature transform. Signature is also differentiable with respect to each data points, and so the backpropagation calculation is available. Thus, the signature can be viewed as a layer in neural network.

3.2 Convolutional Signature Model

CNN, which has been proved to be a powerful tool in computer vision, is an efficient feature extraction technique. This idea has been used in [16] as well as the “**Augment**” module [13], but only 1D CNNs are used.

There are two cases of using 1D CNNs. One case is to extract new sequential features of original paths and then paste them to original path as extra dimensions. This method is not helpful in the high dimensional case. If we use extracted sequential features directly from the 1D CNN, it works as a dimension reduction technique but causes loss of information. With the favor of 2D CNN, we are able to reduce the number of signature features and capture all information in the original path at the same time. Since the convolution here is different from the convolution concept in mathematics, we use the following example to show details of the computation for those who are not so familiar with CNN.

Let $*$ be an operation of element-wise matrix multiplication and summation between two matrices of the same shape $A := (a_{i,j})_{1 \leq i \leq m, 1 \leq j \leq n}$ and $B := (b_{i,j})_{1 \leq i \leq m, 1 \leq j \leq n}$ of the same size:

$$A * B = \sum_{i=1}^m \sum_{j=1}^n a_{i,j} b_{i,j}. \quad (3.1)$$

Suppose the input tensor is $M := (M_{i,j})_{1 \leq i \leq I, 1 \leq j \leq J}$, a kernel window $K := (k_{i,j})_{1 \leq i \leq m, 1 \leq j \leq n}$ and stride window (s, t) , the output $O := (o_{p,q})$ is given by

$$o_{p,q} = (M_{i,j})_{1+(p-1)s \leq i \leq m+(p-1)s, 1+(q-1)t \leq j \leq n+(q-1)t} * K. \quad (3.2)$$

The shape of O depends on how we treat the boundary specifically and does not play a crucial role here, and so we omit it.

Example 3.1 (2D CNN). Let us consider a tensor $M := (M_{i,j})_{1 \leq i,j \leq 5}$ and a kernel window $K := (k_{i,j})_{1 \leq i,j \leq 3}$,

$$M := \begin{pmatrix} 2 & 1 & 0 & 2 & 0 \\ 0 & 1 & 2 & 2 & 1 \\ 0 & 0 & 0 & 1 & 1 \\ 2 & 0 & 0 & 2 & 2 \\ 0 & 2 & 0 & 1 & 1 \end{pmatrix}, \quad \text{and} \quad K := \begin{pmatrix} 0 & 1 & 0 \\ 1 & 0 & -1 \\ -1 & -1 & -1 \end{pmatrix}, \quad \text{respectively,}$$

and a stride window $(1, 1)$. The output will be a 3×3 tensor, denoted by $O = (o_{ij})_{1 \leq i, j \leq 3}$, where each element $o_{i,j}$ of O is given by the element-wise multiplication and summation of $\widetilde{M}^{i,j} := (M_{k,\ell})_{i \leq k \leq i+2, j \leq \ell \leq j+2}$ and K , i.e., $o_{i,j} = \widetilde{M}^{i,j} * K$ for $1 \leq i, j \leq 3$. For example,

$$o_{11} = \begin{pmatrix} 2 & 1 & 0 \\ 0 & 1 & 2 \\ 0 & 0 & 0 \end{pmatrix} * \begin{pmatrix} 0 & 1 & 0 \\ 1 & 0 & -1 \\ -1 & -1 & -1 \end{pmatrix} = 2 \cdot 0 + 1 \cdot 1 + 0 \cdot 0 + \dots + 0 \cdot (-1) = -1,$$

$$o_{12} = \begin{pmatrix} 1 & 0 & 2 \\ 1 & 2 & 2 \\ 0 & 0 & 1 \end{pmatrix} * \begin{pmatrix} 0 & 1 & 0 \\ 1 & 0 & -1 \\ -1 & -1 & -1 \end{pmatrix} = 1 \cdot 0 + 0 \cdot 1 + 2 \cdot 0 + \dots + 1 \cdot (-1) = -2,$$

$$o_{13} = \begin{pmatrix} 0 & 2 & 0 \\ 2 & 2 & 1 \\ 0 & 1 & 1 \end{pmatrix} * \begin{pmatrix} 0 & 1 & 0 \\ 1 & 0 & -1 \\ -1 & -1 & -1 \end{pmatrix} = 1,$$

$$o_{21} = \begin{pmatrix} 0 & 1 & 2 \\ 0 & 0 & 0 \\ 2 & 0 & 0 \end{pmatrix} * \begin{pmatrix} 0 & 1 & 0 \\ 1 & 0 & -1 \\ -1 & -1 & -1 \end{pmatrix} = -1$$

and etc. Therefore, the output O is given by

$$O = \begin{pmatrix} -1 & -2 & 1 \\ -1 & -1 & -1 \\ 0 & -5 & -3 \end{pmatrix}.$$

The Convolutional Signature model uses 2D CNN before the signature transform, and the structure of the convolutional signature model can be described in Figure 2. The convolution is implemented in channels. Since signature is efficient in the time direction, we do not have to convolute the time direction.

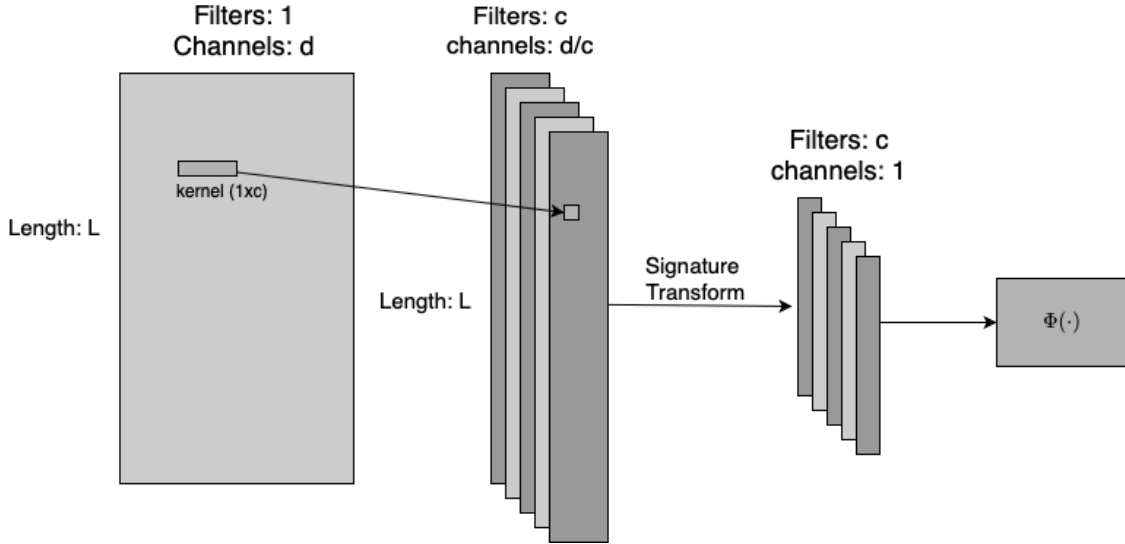


Figure 2: Convolutional neural network and signature transform connected by .

3.3 Number of Features

Suppose $c (\leq d)$ is an integer such that d is divisible by c . Let us fix the ratio $\gamma = \frac{d}{c} \in \mathbb{N}$. For explanation simplicity, we explain the number of features with kernel window of size $(1 \times c)$ and stride $(1 \times c)$. We illustrate our idea in the following example.

Example 3.2. Let us consider a tensor $M := (M_{i,j})_{1 \leq i \leq 5, 1 \leq j \leq 4}$ and 2 kernel windows $K_1 := (k_i^1)_{1 \leq i \leq 2}$, $K_2 := (k_i^2)_{1 \leq i \leq 2}$,

$$M := \begin{pmatrix} 2 & 1 & 0 & 2 \\ 0 & 1 & 2 & 2 \\ 0 & 0 & 0 & 1 \\ 2 & 0 & 0 & 2 \\ 0 & 2 & 0 & 1 \end{pmatrix}, \quad K_1 := \begin{pmatrix} -1 & 1 \end{pmatrix} \quad \text{and} \quad K_2 := \begin{pmatrix} 1 & 2 \end{pmatrix}.$$

By using a stride window (1, 2), we have the output $O = \{O_1, O_2\}$, $O_l = (o_{i,j}^l)_{1 \leq i \leq 5, 1 \leq j \leq 2}$. The computation is done in the same way as Example 3.1, we show several example below:

$$\begin{aligned} o_{1,1}^1 &= (2, 1) * (-1, 1) = -2 + 1 = -1, \\ o_{2,2}^1 &= (2, 2) * (-1, 1) = -2 + 2 = 0, \\ o_{1,1}^2 &= (2, 1) * (1, 2) = 2 + 2 = 4, \\ o_{2,2}^2 &= (2, 2) * (1, 2) = 2 + 4 = 6. \end{aligned}$$

Therefore, the output O is given by

$$O_1 = \begin{pmatrix} -1 & 2 \\ 1 & 0 \\ 0 & 1 \\ -2 & 2 \\ 2 & 1 \end{pmatrix}, \quad O_2 = \begin{pmatrix} 4 & 4 \\ 2 & 6 \\ 0 & 2 \\ 2 & 4 \\ 4 & 2 \end{pmatrix}.$$

In this example, since K_1 and K_2 are linear independent, we can fully recover the input M given K_1, K_2 and output O .

Notice that since the first term in signature transform is always 1, we can omit that. As shown in Figure 2, we start from one d -dimensional path with length L , by using such a convolutional layer, and we are resulted in c paths with each of $\frac{d}{c}$ -dimensional. Then we augment each path with extra time dimension and apply signature transform to each path truncated at depth m , which gives us the number of features

$$N_f := c \cdot \frac{(d/c + 1)^{m+1} - d/c - 1}{d/c + 1 - 1} = \frac{(\gamma + 1)^{m+1} - \gamma - 1}{\gamma^2} \cdot d \quad (3.3)$$

many features by concatenating all c filters. These features can be used in any following neural network model. For example, a fully connected neural network in the simplest case, or a recurrent neural network (RNN) if we compute the sequence of the signature transform.

The number N_f of features grows linearly in d by increasing c linearly and fixing γ . Instead of optimizing this N_f by setting $\gamma = \arg \min N_f$ directly, we can think γ as a hyperparameter to be tuned to avoid overfitting problem. It can be easily seen that by setting $\gamma = 1$, we reach a minimum of N_f when $m \geq 3$. However, lower γ will give us higher c , which increase the number of parameters in CNN step. We consider the sum of number of features and the number of parameters in CNN $N_f + (\frac{d}{\gamma})^2$. Moreover, we can add a multiplier α to the second term, and then define a regularized number on γ ,

$$N^\alpha(\gamma) := \frac{(\gamma + 1)^m - 1}{\gamma^2} \cdot (\gamma + 1) \cdot d + \alpha \cdot \frac{d^2}{\gamma^2}. \quad (3.4)$$

We can set a large α . This will help us avoid overfitting problem, when we are worried about that the CNN layer fits original path too well.

3.4 One-to-one Mapping

Under setup in Section 3.3, we can generalize Example 3.2 and prove such a convolutional layer preserves all information of original path. Suppose that $\{k^i\}_{i=1}^c$ are all c convolutional kernels with $k^i = (k_1^i, \dots, k_c^i)$ for $i = 1, \dots, c$. Denote the square matrix

$$\mathbf{K} := \begin{pmatrix} k_1^1 & \dots & k_c^1 \\ \vdots & \vdots & \vdots \\ k_1^c & \dots & k_c^c \end{pmatrix}.$$

Let the original path be

$$\mathbf{x} = (x_{t_1}, \dots, x_{t_n})^T, \quad x_{t_j} = (x_{t_j}^1, \dots, x_{t_j}^d)$$

and the output path $\{\tilde{x}_i\}_{i=1}^c$, where $\tilde{x}_i = (\tilde{x}_{t_1,i}, \dots, \tilde{x}_{t_n,i})^T$ with $\tilde{x}_{t_j,i} = (\tilde{x}_{t_j,i}^1, \dots, \tilde{x}_{t_j,i}^\gamma)$, $1 \leq i \leq c$. The CNN layer can be represented in equation as

$$\mathbf{K} \cdot (x_{t_j}^{lc+1}, \dots, x_{t_j}^{(l+1)c})^T = (\tilde{x}_{t_j,1}^l, \dots, \tilde{x}_{t_j,c}^l)^T, \quad 1 \leq l \leq \gamma, 1 \leq j \leq n.$$

Lemma 3.1. *If \mathbf{K} is of full rank, then this CNN layer is an one-to-one map.*

Proof. Since \mathbf{K} is square and of full rank, it's invertible.

$$(x_{t_j}^{lc+1}, \dots, x_{t_j}^{(l+1)c})^T = \mathbf{K}^{-1} \cdot (\tilde{x}_{t_j,1}^l, \dots, \tilde{x}_{t_j,c}^l)^T, \quad 1 \leq l \leq \gamma, 1 \leq j \leq n.$$

It follows that \mathbf{x} can be fully recovered by $\tilde{x} := \{\tilde{x}_i\}_{i=1}^c$. □

We denote the CNN layer transform as $\mathbf{K} : \mathcal{V}^1([0, T], \mathbb{R}^d) \rightarrow \mathcal{V}^1([0, T], \mathbb{R}^{d/c+1})^c$. Here, plus 1 in the dimension comes from the time dimension we add to each convoluted paths.

Suppose $f : \mathcal{V}^1([0, T], \mathbb{R}^d) \rightarrow \mathbb{R}$ is the continuous function we need to estimate. Then we have the following theorem.

Theorem 3.1. *Let K be a compact set in $\mathcal{V}^1([0, T], \mathbb{R}^d)$. There exist a CNN layer \mathbf{K} , a neural network model Φ and an integer m such that for any $\epsilon > 0$,*

$$\sup_{x \in K} |f(x) - \Phi \circ S^m \circ K(x)| < \epsilon.$$

Proof. For $\forall x \in \mathcal{V}^1([0, T], \mathbb{R}^d)$,

$$f(x) = f(\mathbf{K}^{-1}(\tilde{x})) = f \circ \mathbf{K}^{-1}(\tilde{x}) := h(\tilde{x}). \quad (3.5)$$

It follows that h is a continuous function. Since $S(\tilde{x}_i)$ is a geometric rough path and characterize the path \tilde{x}_i uniquely for each $1 \leq i \leq c$, there exist a continuous function $\hat{h} : (S(\mathcal{V}^1([0, T], \mathbb{R}^{d/c+1})))^c \rightarrow \mathbb{R}$ such that

$$h(\tilde{x}) = \hat{h}(S(\tilde{x}_1), \dots, S(\tilde{x}_c)).$$

We define $H_i := \left| \hat{h}(S_1^{m_1}(\tilde{x}_1), \dots, S_{i-1}^{m_{i-1}}(\tilde{x}_{i-1}), S(\tilde{x}_i), \dots, S(\tilde{x}_c)) - \hat{h}(S_1^{m_1}(\tilde{x}_1), \dots, S_{i-1}^{m_{i-1}}(\tilde{x}_{i-1}), S_i^{m_i}(\tilde{x}_i), \dots, S(\tilde{x}_c)) \right|$ for $1 \leq i \leq c$. For any $\epsilon > 0$, there exist $\{m_1, \dots, m_c\}$ such that $H_i \leq \frac{\epsilon}{2c}$ for all $1 \leq i \leq c$ by the continuity of \hat{h} and the factorial decay property of signature, see Example 2.2.

Set $m = \max\{m_1, \dots, m_c\}$, we have

$$\left| \hat{h}(S(\tilde{x}_1), \dots, S(\tilde{x}_c)) - \hat{h}(S^m(\tilde{x}_1), \dots, S^m(\tilde{x}_c)) \right| \leq \sum_{i=1}^c H_i \leq \frac{\epsilon}{2}. \quad (3.6)$$

This \hat{h} is not necessary linear because there might be some dependence among $\{\tilde{x}_i\}_{i=1}^c$, but it can be approximated by a neural network model arbitrarily well. A wide range of Φ can be chosen. For example, a fully connected shallow neural network with one wide enough hidden layer and some activation function would work, see [9]. That is, there exists Φ such that

$$\left| \Phi(S^m(\tilde{x}_1), \dots, S^m(\tilde{x}_c)) - \hat{h}(S^m(\tilde{x}_1), \dots, S^m(\tilde{x}_c)) \right| \leq \frac{\epsilon}{2}. \quad (3.7)$$

By combining (3.5), (3.6), (3.7) together, we get the desired result. \square

In CNN-Sig model, CNN layer can be understood as data dependent encoder which help us find the best way of encoding original path to several lower dimensional paths. On one hand, a large c will result in overfitting problem of CNN layer. On the other hand, small c will produce large number of features for Φ , and then Φ may has the overfitting problem. This tradeoff can be balanced by minimizing $N^\alpha(\gamma)$ in equation (3.4). Thus, although the choice of c does not affect the universality of the model, it could help with resolving the overfitting problem. In most of experiments in Section 4, we use $c = d/2$ to get a better result.

Remark 3.1. *When we do experiments of CNN-Sig model, this model works even better compare to plain signature transform of original path on testing data, it is because CNN-Sig reduces the number of features and thus overcome the overfitting problem better than direct signature transform.*

Moreover, the signature transform can be done in a sequential way. Then we can choose a RNN model (GRU or LSTM) for Φ . Some other candidates for Φ can be Attention model like Transformer, 1d-CNN and so on, which might help us get better predictions. This CNN-Sig model is very flexible and can be incorporated with many other well developed deep learning model as Φ , which depends specifically on the task. In practice, we can use a different stride size to allow some overlap during convolution and reduce the number of filters. The one-to-one mapping property may be lost in this case if we choose small number of filters, but it results in less overfitting. Another alternative is that we can also convolute over time dimension, provided that correlation over time is of importance to the sequential data.

4 Experiments

4.1 Classification of GARCH Time Series

The generalized autoregressive conditional heteroskedasticity (GARCH) process is usually used in econometrics to describe the time-varying volatility of financial time series [8, 4]. GARCH provides a more real-world context than other models when predicting the financial time series, compare to other time series model like ARIMA. We apply logistic regression to Example 2.3, i.e. the goal is to estimate $g(S^m(x)) = (\hat{p}_0, \hat{p}_1)$ in (2.4), where

$$\log \frac{\hat{p}_1}{1 - \hat{p}_1} = \langle l, S^m(x) \rangle, \quad (4.1)$$

subject to $\hat{p}_0 + \hat{p}_1 = 1$, l is a linear functional on $T^m(\mathbb{R}^d)$ to be chosen such that the cross entropy

$$E(l) = - \sum_{i=1}^N (y^i \log \hat{p}^i + (1 - y^i) \log(1 - \hat{p}^i)) \quad (4.2)$$

is minimized, and we predict labels by $\hat{y}^i = \arg \max_i \hat{p}_i$. 500 samples are generated for each class and we use 70% of each class as training data and 30% of each as testing data. By using $m = 4$, we get training accuracy 96.4% and testing accuracy 97.0%. The confusion matrix is given below in Table 2.

		Predicted	
True	0	343	7
	1	18	332

		Predicted	
True	0	147	3
	1	6	144

Table 2: Training (left) and testing (right) confusion matrices.

4.2 Classification Problem By Signature: Directed Chain Discrete Time Series

In [7], authors proposed a particle system of diffusion processes, coupled through a chain-like directed graph. We discuss one of their detection problem examples here. In Remark 4.5 of [7], a discrete time analogue of the mean-reverting type, directed chain model with mean-field type interaction is proposed. More specifically, we have a discrete-time time series $\{X_n\}_{n \geq 1}$ and $\{\tilde{X}_n\}_{n \geq 1}$. Each X_n is coupled with its neighborhood \tilde{X}_n , the parameter $u \in [0, 1]$ measures how much X_n depends on its neighborhood. Because of the mean-field interaction, X and \tilde{X} have the same distribution given by (4.3).

$$X_n = \sum_{0 \leq l \leq k \leq n-1} \binom{k}{l} u^l (1-a)^l a^{k-l} \epsilon_{n-k,l}, \quad \tilde{X}_n = \sum_{0 \leq l \leq k \leq n-1} \binom{k}{l} u^l (1-a)^l a^{k-l} \epsilon_{n-k,l+1}, \quad n \geq 1. \quad (4.3)$$

Suppose that our only observation is $\{X_n\}_{n \geq 1}$, but both $\{\tilde{X}_n\}_{n \geq 1}$ and u are hidden to us. Our question is that given the access to $\{X_n\}_{n \geq 1}$ generated by different u , can we determine their classes?

In this part, we first set the default parameters and generate training and testing paths according to (4.3). First we initial some parameters: $a = 0.5$, $u = 0.2$ or 0.8 for classification task, $N = 100$ is the time steps, $1/N$ is the variance of ϵ .

In order to generate paths, we generate a $n \times (n+1)$ matrix \mathcal{E} of the error terms ϵ , and then pick the column we need for each n . The summation takes time $O(N^2)$ and we have to range n from 1 to N . The time complexity is the order of $O(N^3)$. We simulate 2000 training paths and 400 testing paths for this task.

Method 1: Logistic Regression

In this part, we use 2000 training paths, 1000 for $u = 0.2$ and 1000 for $u = 0.8$. And then we calculate the signature transform of these paths, augmented with time dimension, up to degree 9.

We build a Logistic Regression model on the signatures of training data and test this model, see equation (4.1).

The result is shown in table 3. We can see that this is a positive result, which indicates that signature does capture useful features for u in these special time series.

Training Acc	Testing Acc
0.7465	0.7375

Table 3: Training accuracy and testing accuracy on Logistic regression.

Method 2: Deep Neural Network

We build a Neural Network model in order to get a better result. We use 4 hidden layers with 256, 256, 128, 2 units respectively. For first 3 layers, we use "ReLU" as activation function, for last layer, we use "Softmax" activation function as the approximated probability values. After training for 20 epochs, the result is shown in table 4.

This 4 layer neural network model produces better accuracy than logistic regression. The reason follows Remark 2.2. Logistic regression trains a linear classifier, but it cannot be used to estimate $p(\cdot)$ efficiently because $p(\cdot)$ is not continuous in x . This DNN model add nonlinearity to $g(\cdot)$ and hence works better.

Training Acc	Testing Acc
0.8930	0.8925

Table 4: Training accuracy and testing accuracy on NN.

4.3 High Dimensional Time Series

Signature is an efficient tool as a feature map for high frequency sequential data to reduces the number of features. However, the number of signature terms increases exponentially as dimension (or channels in the language of PyTorch) increasing. In Section 3, we proposed the CNN-Sig model to address this problem.

Experiments - Regression Problem for Maximum-Call Payoff

We investigate our model on a high-dimension European type maximum call option. In other words, we want to use our CNN-Sig model to estimate the payoff

$$\max_{1 \leq k \leq d} ((X_T^k - K)^+),$$

where T is terminal time, K is strike price, superscript k represents the k -th coordinate of this d -dimension path. If X_T^k is smaller than K for all $1 \leq k \leq d$, this payoff is zero. Otherwise the payoff would be the maximum of $(X_T^k - K)$ over those k satisfies $X_T^k \geq K$. Result of this experiment may motivate us to use CNN-Sig model in high dimensional optimal stopping problem from financial mathematics.

Because of the limitation of exponential growth in the number of features, we use lower $d = 6, 10, 12, 20$ to compare the performance between plain signature transform and CNN-Sig model. Then we apply this model to test its performance with higher dimension $d = 50$.

d	Sig+LR				CNN-Sig			
	Training		Testing		Training		Testing	
	MAE	R^2	MAE	R^2	MAE	R^2	MAE	R^2
6 ($\gamma = 2$)	0.001	1.000	0.101	0.538	0.020	0.986	0.030	0.972
10($\gamma = 2$)	0.000	1.000	0.124	0.806	0.033	0.988	0.062	0.962
12($\gamma = 2$)	0.000	1.000	0.153	0.821	0.048	0.981	0.111	0.924
20($\gamma = 1$)	0.000	1.000	0.225	0.838	0.177	0.916	0.203	0.892

Table 5: Training and testing mean absolute error(MAE) and R^2 for direct signature transform plus linear regression(Sig+LR) and CNN-Sig model with Φ as a fully connected neural network.

We generate 1000 training paths and 1000 testing paths for cases of $d = 6, 10, 12$, and generate 3000 training paths and 1000 testing paths for case $d = 20$.

For all 4 cases, we consider $m = 4$ as the signature depth. For Φ in CNN-Sig model, we use the same structure, 2 fully connected layers followed by ReLu activation function and then a fully connected layer. We didn't apply any technique for avoiding overfitting problem in CNN-Sig model to make this comparison fair. The result for comparison is shown in table 5. We can see that for all these 4 cases, CNN-Sig model beat direct signature transform. Since CNN-Sig model reduce the number of features, it can help avoid overfitting problem compare to Sig+LR. We produce the QQ plots for training and testing results of CNN-Sig model, see Figure 3.

For $d = 50$, we use the same CNN-Sig structure as lower d cases for training. The training MAE is 0.206 with $R^2 = 0.982$ and testing MAE is 0.751 with $R^2 = 0.797$. The QQ plot of training and testing results is in Figure 4.

Experiments - Classification

We did experiments for different datasets from [2]. Each of them is of high dimension and contains multiple classes. The results are listed in table 6.⁴ CNN-Sig model works very well on PERMS dataset, which is of dimension 963, and the training speed is fast compare to kernel methods in [26]. By the discussion in Section 4.3, we can also expect a descent result for CNN-Sig model on lower dimensional time series, say $5 \leq d \leq 20$. We can see from Table 6 that CNN-Sig model works very well on ArabicDigits and Japanese Vowels datasets, which are of dimension 13 and 9 respectively.

4.4 Sentiment Analysis by Signature

In Natural Language Processing (NLP), text sentence can be regarded as sequential data. A conventional way to represent words is using high dimensional vector, which is called word embedding. These kind of word embedding is usually of 50, 100, 300

⁴All these computations are done via Google Colab free version.

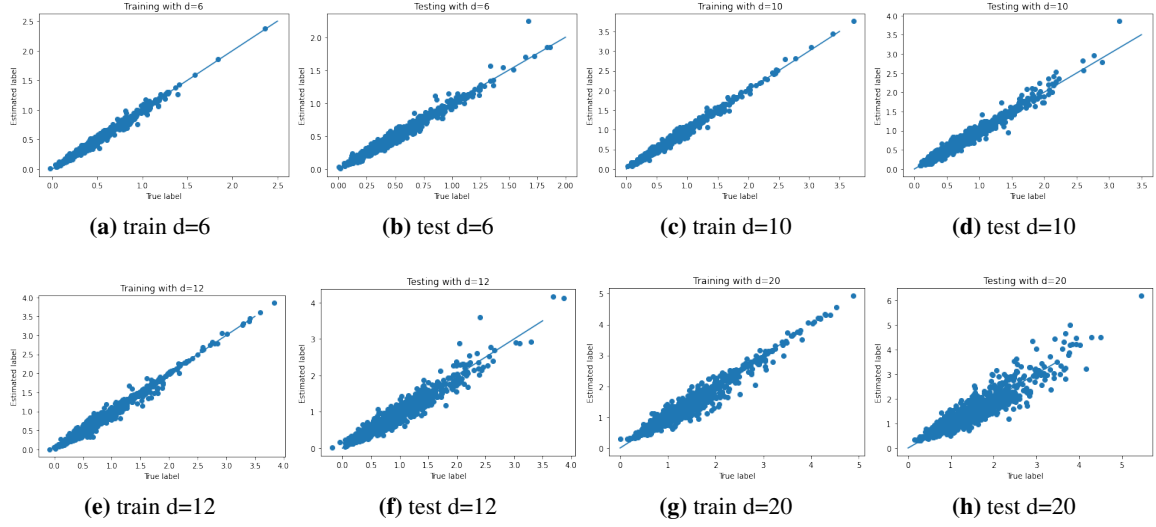


Figure 3: QQ plot for training and testing result for lower dimensional regression with $d = 6, 10, 12, 20$ using CNN-Sig model.

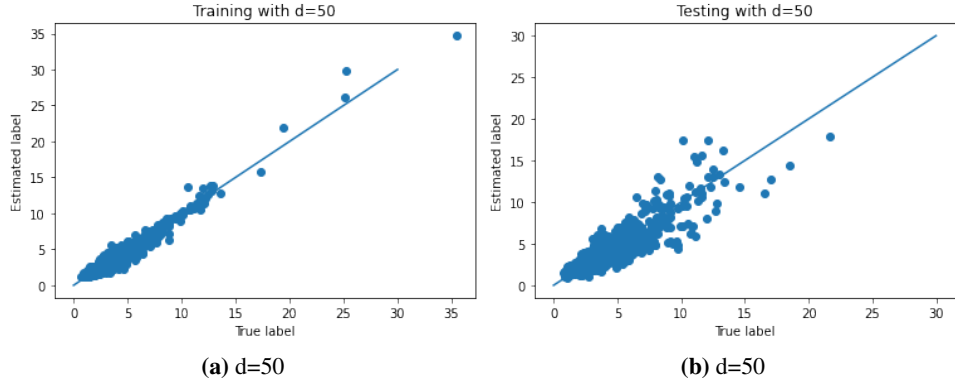


Figure 4: QQ plot for training and testing result for regression task with $d = 50$ using CNN-Sig model.

dimension. Using plain signature transform becomes extremely difficult because of these high dimensions. We apply our previous proposed CNN-Sig model to address this problem. The dataset we use is IMDB movie reviews, [22].

This IMDB dataset contains 50,000 movie reviews, each of them is labelled by either "pos" or "neg", which represent **Positive** for **Negative** respectively. The IMDB dataset is split into training and testing evenly. For training part, we use 17500 samples for training the model, and use the other 7500 samples as validation dataset. A 100-dimension word embedding GloVe 100d [24] is used as the initial embedding, this high dimension restrict us to use plain signature transform. In our model, by setting γ to be small, we use 1 convolutional 2d layer to reduce the dimension from 100 to c paths with each of $\gamma + 1$ dimensional augmented by extra time dimension. It means the number of signature features is reduced from $\sum_{k=1}^m 100^m$ to N_f . Given $m = 4$ and $\gamma = 2$, we reduced the number from 101,010,100 to $N_f = 6000$. Φ we used here is a 2 layer fully connected neural network with ReLu function as the activation. The architecture is shown in Figure 5.

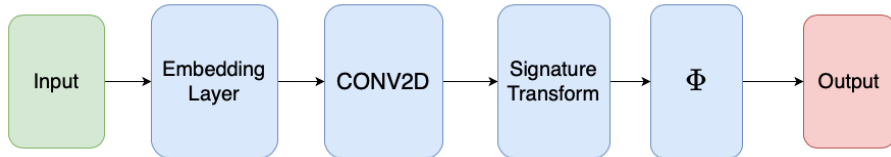


Figure 5: Convolutional Signature neural network model for IMDB dataset.

The result is shown in Table 7 and the testing accuracy has been improved to **88.65%** which is higher than the result in [26] (83%).

Datasets	dim	classes	train/test size	training acc	testing acc	time (sec)
ArabicDigits	13	10	6600/2200	0.996	0.968	485.5
AUSLAN	22	95	1140/1425	1.000	0.808	209.14
CMU MOCAP	62	2	29/29	1.000	1.000	22.5
Japanese Vowels	12	9	270/370	1.000	0.968	21.6
Kick vs Punch	62	2	16/10	1.000	1.000	59.2
PERMS	963	7	267/173	0.993	0.838	143.8
Walk vs Run	62	2	28/16	1.000	1.000	37.9

Table 6: High dimensional time series data for classification problem.

Training Acc	Valid Acc	Testing Acc
91.78%	89.46%	88.65%

Table 7: Training accuracy, validation accuracy and testing accuracy on IMDB dataset.

We believe that by applying more complicated structure, such as using attention model for Φ and a sliding window, e.g., see [23], for calculating a sequential signature transform, the accuracy can be improved.

5 Conclusion

Using signature to summarize sequential data has been proved to be very efficient in the low dimensional cases. However, signature transform suffers from exponential growth of the number of features with respect to the path dimension. This makes both regression and classification problem impossible in practical.

In this paper, we proposed a Convolutional Signature (CNN-Sig) model to address this problem. By using a convolutional layer, we achieve a linear growth of the number of features and preserve all information simultaneously. The experiments show that this model can be a good candidate for classifying multi-dimension sequential data. Moreover, signature has been proved experimentally to be insensitive to missing values, this property may be useful in many NLP tasks. CNN-Sig model can address the high dimension problem and provides a possible way to apply signature transform in NLP tasks.

References

- [1] ARRIBAS, I. P. Derivatives pricing using signature payoffs, Preprint available at <https://arxiv.org/abs/1809.09466> (2018).
- [2] BAYDOGAN, M. *Multivariate Time Series Classification Datasets*, 2015. <http://mustafabaydogan.com>, [Accessed: 2020-07-12].
- [3] BOEDIHARDJO, H., GENG, X., LYONS, T., AND YANG, D. The signature of a rough path: Uniqueness, *Advances in Mathematics*, 293 (2014) 720–737.
- [4] BOLLERSLEV, T. Generalized autoregressive conditional heteroskedasticity. *Journal of Econometrics* 31, 3 (1986), 307–327.
- [5] CHEVYREV, I., AND LYONS, T. Characteristic functions of measures on geometric rough paths. *The Annals of Probability* 44, 6 (2016), 4049–4082.
- [6] CHO, K., VAN MERRIENBOER, B., GULCEHRE, C., BOUGARES, F., SCHWENK, H., AND BENGIO, Y. Learning phrase representations using rnn encoder-decoder for statistical machine translation. In *Conference on Empirical Methods in Natural Language Processing (EMNLP 2014)* (2014).
- [7] DETERING, N., FOUQUE, J.-P., AND ICHIBA, T. Directed chain stochastic differential equations, *Stochastic Processes and their Applications*, 130 (2020), 2519–2551.
- [8] ENGLE, R. F. Autoregressive conditional heteroscedasticity with estimates of the variance of united kingdom inflation. *Econometrica: Journal of the Econometric Society* (1982), 987–1007.
- [9] FUNAHASHI, K.-I. On the approximate realization of continuous mappings by neural networks. *Neural Networks* 2, 3 (1989), 183–192.
- [10] GYURKÓ, L. G., LYONS, T., KONTKOWSKI, M., AND FIELD, J. Extracting information from the signature of a financial data stream, Preprint available at <https://arxiv.org/abs/1307.7244> (2013).
- [11] HOCHREITER, S., AND SCHMIDHUBER, J. Long short-term memory. *Neural Comput.* 9, 8 (1997), 1735–1780.
- [12] KIDGER, P., BONNIER, P., PEREZ ARRIBAS, I., SALVI, C., AND LYONS, T. Deep signature transforms. In *Advances in Neural Information Processing Systems 32*. Curran Associates, Inc., (2019), pp. 3105–3115.

-
- [13] KIDGER, P., AND LYONS, T. Signatory: differentiable computations of the signature and logsignature transforms, on both CPU and GPU. Preprint available at <https://arxiv.org/abs/2001.00706> (2020).
 - [14] KIRALY, F. J., AND OBERHAUSER, H. Kernels for sequentially ordered data. *Journal of Machine Learning Research* 20, 31 (2019), 1–45.
 - [15] LEVIN, D. A., LYONS, T., AND NI, H. Learning from the past, predicting the statistics for the future, learning an evolving system. Preprint available at <https://arxiv.org/abs/1309.0260> (2013).
 - [16] LIAO, S., LYONS, T., YANG, W., AND NI, H. Learning stochastic differential equations using rnn with log signature features, Preprint available at <https://arxiv.org/abs/1908.08286> (2019).
 - [17] LYONS, T., NEJAD, S., AND ARRIBAS, I. P. Nonparametric pricing and hedging of exotic derivatives, 2019.
 - [18] LYONS, T., NEJAD, S., AND ARRIBAS, I. P. Numerical method for model-free pricing of exotic derivatives using rough path signatures, Preprint available at <https://arxiv.org/abs/1905.00711> (2019).
 - [19] LYONS, T., NI, H., AND OBERHAUSER, H. A feature set for streams and an application to high-frequency financial tick data. In *Proceedings of the 2014 International Conference on Big Data Science and Computing* New York, BigDataScience '14, Association for Computing Machinery (2014).
 - [20] LYONS, T., QIAN, Z., AND PRESS, O. U. *System Control and Rough Paths*. Oxford mathematical monographs. Clarendon Press, (2002).
 - [21] LYONS, T. J., CARUANA, M., AND LÉVY, T. Differential equations driven by rough paths. In *Differential Equations Driven by Rough Paths: École d'Été de Probabilités de Saint-Flour XXXIV - 2004*, vol. 1908 of *Lecture Notes in Mathematics*. Springer Berlin Heidelberg, Berlin, Heidelberg, (2007), pp. 81–93.
 - [22] MAAS, A. L., DALY, R. E., PHAM, P. T., HUANG, D., NG, A. Y., AND POTTS, C. Learning word vectors for sentiment analysis. In *Proceedings of the 49th Annual Meeting of the Association for Computational Linguistics: Human Language Technologies* Portland, Association for Computational Linguistics, (2011) pp. 142–150.
 - [23] MORRILL, J., FERMANIAN, A., KIDGER, P., AND LYONS, T. A generalised signature method for time series, Preprint available at <https://arxiv.org/abs/2006.00873> (2020).
 - [24] PENNINGTON, J., SOCHER, R., AND MANNING, C. D. Glove: Global vectors for word representation. In *Empirical Methods in Natural Language Processing (EMNLP)* (2014), pp. 1532–1543.
 - [25] RAISSI, M., PERDIKARIS, P., AND KARNIADAKIS, G. E. Numerical gaussian processes for time-dependent and non-linear partial differential equations, Preprint available at <https://arxiv.org/abs/1703.10230> (2017).
 - [26] TOTH, C., AND OBERHAUSER, H. Bayesian learning from sequential data using gaussian processes with signature covariances, Preprint available at <https://arxiv.org/abs/1906.08215> (2019).
 - [27] WILLIAMS, C. K., AND RASMUSSEN, C. E. *Gaussian processes for machine learning*, vol. 2. MIT press Cambridge, MA, (2006).